1

Multiphysics Simulations on the Effect of Fluidic Concentration Profiles Over Y-Channel and T-Channel Designs

Pavar Sai Kumar and Sanket Goel

MEMS, Microfluidics and Nanoelectronics (MMNE) Lab, Department of Electrical and Electronics Engineering, Birla Institute of Technology and Science (BITS) Pilani, Hyderabad Campus, Hyderabad, Telangana, India

1.1 Introduction

Miniaturization of systems and processes has recently gained tremendous interest due to its viable control over countless parameters in chemical reactions, including pressure, temperature, mass transport, and volumes. Further, the microfluidic lab-on-chip devices, manipulating the fluid behaviors at dimensions of less than 1 mm, benefit various applications, including clinical diagnostics, biological and chemical reactions, DNA amplification studies, and biomarker detections [1–3]. The exceptional performance of microfluidics is due to its mixing efficiency for most chemical and biological applications [4–8]. Molecular diffusions are generally used to facilitate desired reactions between more than two fluids at the microfluidic scale. Further, the flow in microscale devices is laminar ($Re < 100$) and needs a micromixer for efficient mixing. However, fluid mixing is not a problem in macro devices owing to the turbulent flow [9].

Microfluidic mixing is classified as either active or passive [10]. Active mixing utilizes external sources, including magnetic beads, acoustic waves, and electric fields. Moreover, active mixers can provide higher mixing efficiencies but are more complex and costly, limiting their incorporation into point-of-care (PoC) devices. By contrast, passive mixing occurs through the advection, and diffusion entirely relies on the microfluidic channel dimension and device designs [11]. The commonly adopted channel designs include serpentine, dynamic focusing, chaotic advection, multiphase flow, creation of obstacles (i.e., grooves, baffles,

Micro Electromechanical Systems (MEMS): Practical Lab Manual, First Edition.
Edited by Sanket Goel.

Published 2025 by John Wiley & Sons, Inc.
Companion website: www.wiley.com/go/goel

curves, and ridges), herringbone, T-shape, Y-shape, pico injections, and flow focusing [12]. However, in order to avoid larger channel lengths and reaction times, passive mixing must be optimized for effective mixings [13, 14]. This chapter reviews a simulation conducted with an active mixer to determine the optimal mix using the Y- and T-shaped channels through the COMSOL.

1.2 Real-Time Applications of This Study

Reza Mahdavi et al. leveraged the COMSOL simulations for organ-on-a-chip microfluidic platforms toward in vitro liver zonation studies (simulate flow rates, cell densities, and cell consumptions) [15]. Similarly, Ashok Kumar Loganathan et al. represented the microfluidic design optimizations for revolutionized blood plasma separation using simulations [16]. Nevertheless, microfluidic simulation plays a vital role in several advanced applications, including gas sensor optimizations [17], engineering of nanoparticles [18], acoustophoresis [19], and single-cell fluid shear stress studies [20].

1.3 Simulation Section

1.3.1 Prerequisites

Windows 10/11 operating system, a minimum of 4 GB RAM, storage of 250 GB, and a licensed version of above or equal to 5.0 COMSOL software.

1.3.2 Computer-Aided Designing (CAD)

CAD modeling and designing are performed in the student-licensed Solidworks 2021 version. The channel dimensions are 1 mm wide for both T and Y-shaped designs. Figure 1.1 shows the representation of the designed CAD models. Further, the designs are saved in .dxf format, allowing for direct import into COMSOL.

1.3.3 Simulation Parameters

Concentration of c1 = 1 mM at inlet 1.

Concentration of c2 = 5 mM at inlet 2.

Velocity of inlet 1 = 2000 µl/min = 0.03334 m/s.

Velocity of inlet 2 = varied as 2000 µl/min = 0.03334 m/s, 1000 µl/min = 0.016667 m/s, 500 µl/min = 0.008333 m/s, 100 µl/min = 0.0016667 m/s.

Time of observation = 0–10 seconds at a step of 0.1 second.

The above parameters are limited to this study; however, users can change and simulate each parametric variation.

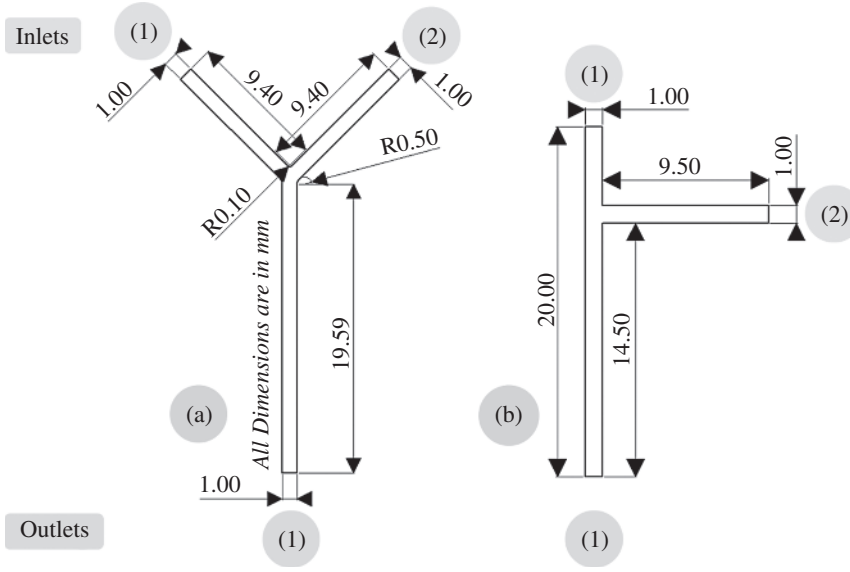

Figure 1.1 CAD images of Y and T-shaped channels (All dimensions are in mm).

1.4 Results and Discussions

1.4.1 Model Designing

Step 1: Use any computeriaided designing (CAD) tool (this case uses SOLIDWORKS 2021).
Step 2: Draw the respective T-shaped and Y-shaped 2D channels, as shown in Figure 1.1.
Step 3: Create an offset or channel width in both designs as 1 mm.
Step 4: Save the respective files individually through the relevant CAD tool extension.
Step 5: Convert the respective saved files to .dxf format individually for easy import into COMSOL.

1.4.2 COMSOL Simulations

In COMSOL, open the new window and select Model Wizard.

Step 1: Click on the default 2D space dimension.
Step 2: Select physics in the search bar and add (i) Transport of diluted species and (ii) Laminar flow.
Step 3: Select the study as Time-dependent (i.e., to study the dependency of results with time) and click done.
Step 4: Change the default dimensions in the popup window of Geometry to "mm."

Step 5: Right-click on the Geometry: import the saved Y-channel.dxf and T-channel.dxf files individually for two studies, respectively.

Step 6: Right-click on the Materials: add the materials from the library (search PDMS and apply as boundary excluding the inlets and outlet, as shown in Figure 1.1; search WATER and apply as domain)

Step 7: Right-click on the Laminar flow: Select inlet and choose the edge as inlet 1, shown in Figure 1.1, and, keeping the boundary condition as velocity, enter the normal inflow velocity values of user-defined, respectively (in this case 2000 µl/min = 0.03334 m/s, 1000 µl/min = 0.016667 m/s, 500 µl/min = 0.008333 m/s, 100 µl/min = 0.0016667 m/s). Repeat the same for inlet 2, respectively. Similarly, right-click on the Laminar flow section, select outlet, and choose the outlet edge, shown in Figure 1.1, respectively, and leave the default settings as it is, P = 0.

Step 8: Click on the transport of diluted species section, and here, the number of dependent variables (i.e., concentrations) can be set. In this case, we set the number of species as 2 and concentrations named c1 and c2.

Step 9: Click on the transport properties to ensure the convection was set to the velocity field.

Step 10: Right-click on the transport of diluted species. Select the concentration, and in the boundary selection, select inlet 1, concentration species c1, and provide the user-defined concentration. In this case, concentration c1 was set to 1 mol/m^3, i.e., 1 mM.

Step 11: Similarly, right-click on the transport of diluted species, select the concentration, provide inlet 2 as the boundary, and select c2, enter a user-defined value. In this case, the c2 was set to 5 mol/m^3, i.e., 5 mM.

Step 12: Meshing: click on the mesh and select the element size depending on the user. In this case, the mesh size was set to fine with physics-controlled default mesh selection and selected build all to process the meshing.

Step 13: Click on the study/step 1-Time dependent: In the study settings, adjust the time unit output times (start, step, end) as (0, 0.1, 10) s. It is, again, user-defined.

Step 14: Compute the study in the time-dependent section and wait until the process is complete to visualize the results.

Step 15: The concentration profiles can be seen in the results section, concentration c1 and concentration c2. Right-click on any one of the concentrations c1 or c2 and click duplicate.

Step 16: In the duplicated concentration, select the surface and change the expression to max(c1, c2) such that the simultaneous fluid interactions can be visualized during the animation of the file. Also, the mixing pattern can be seen effectively.

Step 17: Right-click on the duplicated concentration: select the arrow surface, adjust the coloring arrow positioning (in this case, set to 20 for each of *x* and *y*), and click plot.

Step 18: Click the results section in the main toolbar, click Animation Player to visualize the fluid interactions from the set time of 0–10 seconds, or select the animation file to export the animations.

Step 19: Click on the selected animation, and the player (on, off, and pause) can be seen in the top left corner of the graphics window. Click on the play, then the COMSOL simulates the data and plays the graphics.

Step 20: In the animation settings, change the target to file to export as user-defined formats (i.e., gif, avi).

Step 21: Each time the inlet velocities or concentrations change, the study must be computed to reflect the same in the results section.

Step 22: Right-click on the export: Images, plots, or data, if any, can be exported from here.

Step 23: Right-click on the reports: select the type of report (brief, intermediate, or complete) that can be exported at desired locations.

Step 24: Save the COMSOL simulated file for future modifications and close the simulations.

Table 1.1 shows the simulations performed by varying the velocity of inlet 2 as 2000 µl/min, 1000 µl/min, 500 µl/min, and 100 µl/min at a fixed velocity of inlet 1 as 2000 µl/min. However, it is user-defined and can be adjusted depending on the requirements.

In this study, the concentrations of the c1 and c2 were fixed during the change velocity studies. However, this also can be varied depending on the requirement and simulated.

As shown in Table 1.1, both the Y-channel and T-channel exhibit similar behaviors, including at the same flow rates of inlet 1 and 2 (2000 µl/min each). It can be observed that the mixing profile of both fluids was aligned in the middle of the outlet channel, and the labeling provided on the right side of the image shows the concentrations at each level at 10th seconds.

Moreover, decreasing the velocity of inlet 2 shows the right side shift of fluid alignment and the concentration changes, which could be seen from the label provided.

It was observed that the lower flow rates of inlet 2 with concentration c2 at 5 mM could mix effectively with the higher flow rate of inlet 1 with concentration c1 at 1 mM. Also, the mixing profile indicates that the 5 mM was consumed to ~2.5 mM after mixing at 10th seconds. However, if the path length of the channel increases, then the complete consumption can be seen.

Table 1.1 Y- and T-channel simulations with a varying flow rate of Inlet 2 (fixed concentrations of c1 = 1 mM, c2 = 5 mM, and time at 10th seconds).

Channel type	Inlets		Images
	1	2	
	Flowrate (µl/min)		
Y-channel	2000	2000	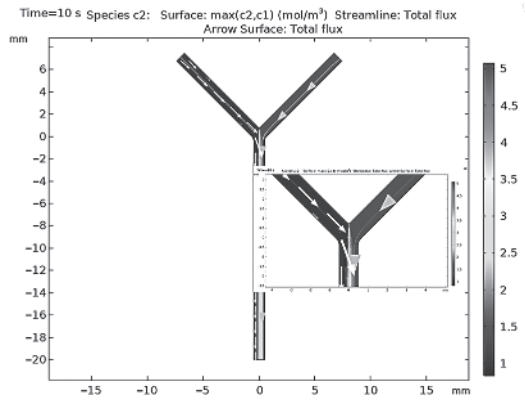
	2000	1000	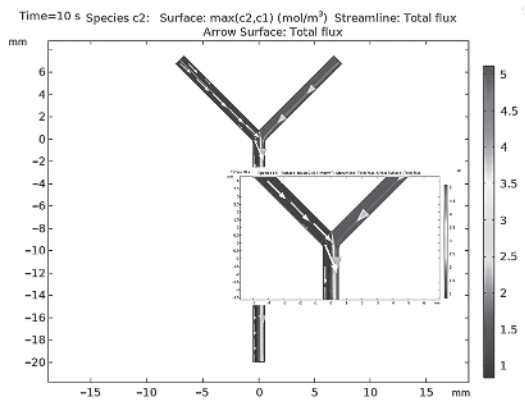

Table 1.1 (Continued)

Channel type	Inlets	Images
	2000 500	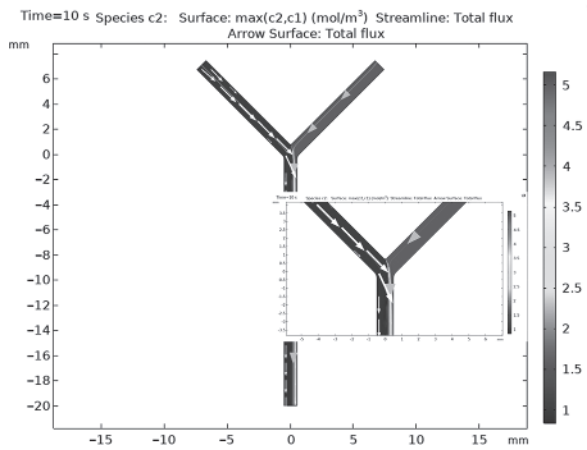
	2000 100	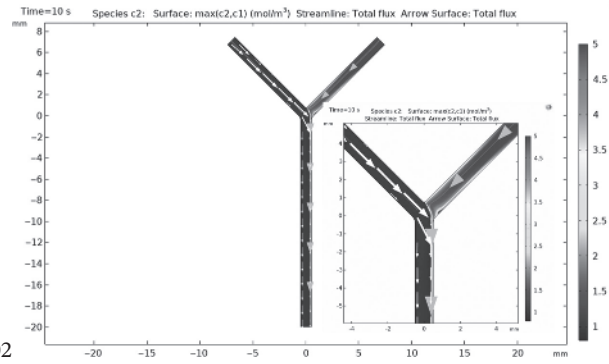
	02	

(*Continued*)

Table 1.1 (Continued)

Channel type	Inlets		Images
T-channel	2000	2000	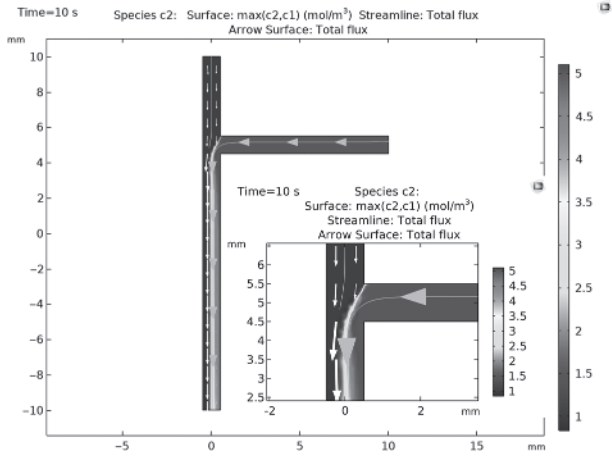
	2000	1000	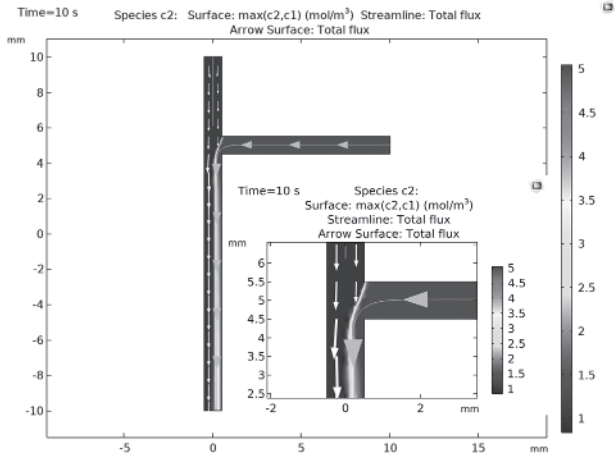

Table 1.1 (Continued)

Channel type	Inlets	Images
	2000 500	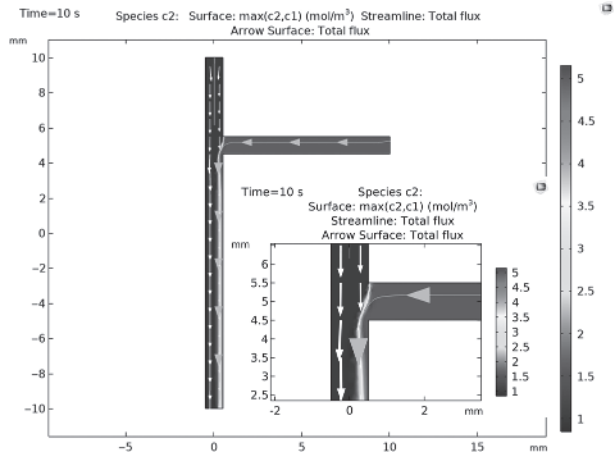
	2000 100	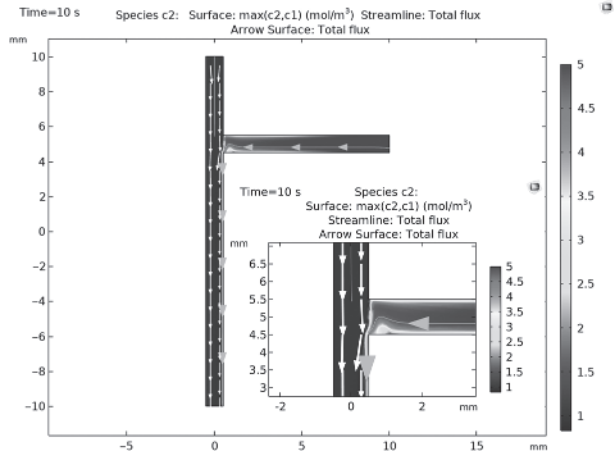

1.5 Conclusion

Y- and T-channel designs were simulated to observe the change in the concentration profiles with varying flow rates. The flow rates or velocities of inlets significantly impact the mixing profiles of concentrations. This study observed that the lower flow rates of inlet 2 facilitated the increased mixing at 10th seconds than the higher flow rates. It was also shown that users can change the concentration parameters, velocity parameters, and the time of observation to obtain significant and specific simulations.

References

1 Hama, B., Mahajan, G., Fodor, P.S. et al. (2018). Evolution of mixing in a microfluidic reverse-staggered herringbone micromixer. *Microfluid. Nanofluidics* 22 (5): 54. https://doi.org/10.1007/s10404-018-2074-0.

2 Singh, R.K., Kumar, P.S., Amreen, K. et al. (2022). Disposable miniaturized electrochemical sensing platform with laser-induced reduced graphene oxide electrodes for multiplexed biochemical analysis. *IEEE Trans. Nanobiosci.* 1. https://doi.org/10.1109/TNB.2022.3216312.

3 Wagh, M.D., Renuka, H., Kumar, P.S. et al. (2022). Integrated microfluidic device with MXene enhanced laser-induced graphene bioelectrode for sensitive and selective electroanalytical detection of dopamine. *IEEE Sens. J.* 22 (14): 14620–14627. https://doi.org/10.1109/JSEN.2022.3182293.

4 Jung, Y., Hyun, J., Choi, J. et al. (2017). Manipulation of cells' position across a microfluidic channel using a series of continuously varying herringbone structures. *Micro Nano Syst. Lett.* 5 (1): 6. https://doi.org/10.1186/s40486-016-0040-8.

5 Singh, R.K., Kumar, P.S., Amreen, K. et al. (2023). Miniaturized paper based sensor with reduced graphene oxide as interdigitated electrodes for multiple applications. *IEEE Sens. J.* 23 (13): 14950–14956. https://doi.org/10.1109/JSEN.2023.3277800.

6 Kumar, P.S., Madapusi, S., and Goel, S. (2023). 3D printed microfluidic chemiluminescence PoC device with self-powering and integrated incubating system: validation via ALP detection on disposable μPADs. *Microchem. J.* 189: 108518. https://doi.org/10.1016/j.microc.2023.108518.

7 Kumar, P.S., Advincula, P., and Goel, S.G. (2022). First report on onsite temperature based recovery of quenched chemiluminescence signal from graphenized μPADs: validation by catechins radical scavenging. *Nano Futur.* https://doi.org/10.1088/2399-1984/ac9d78.

8 Kumar, P.S., Bhand, S., Das, A.K., and Goel, S. (2022). Microfluidic paper device with on-site heating to produce reactive peroxide species for enhanced smartphone enabled chemiluminescence signal. *Talanta* 236: 122858. https://doi.org/10.1016/j.talanta.2021.122858.

9 Julius, L.A.N., Jagannadh, V.K., Michael, I.J. et al. (2016). Design and validation of on-chip planar mixer based on advection and viscoelastic effects. *Biochip J.* 10 (1): 16–24. https://doi.org/10.1007/s13206-016-0103-1.

10 Le The, H., Ta, B.Q., Le Thanh, H. et al. (2015). Geometric effects on mixing performance in a novel passive micromixer with trapezoidal-zigzag channels. *J. Micromech. Microeng.* 25 (9): 94004. https://doi.org/10.1088/0960-1317/25/9/094004.

11 Shah, I., Kim, S.W., Kim, K. et al. (2019). Experimental and numerical analysis of Y-shaped split and recombination micro-mixer with different mixing units. *Chem. Eng. J.* 358: 691–706. https://doi.org/10.1016/j.cej.2018.09.045.

12 Mansour, M. et al. (2017). Numerical study of liquid-liquid mixing in helical pipes. *Chem. Eng. Sci.* 172: 250–261. https://doi.org/10.1016/j.ces.2017.06.015.

13 Kumar, P.S., Madapusi, S., and Goel, S. (2023). Sub-second synthesis of silver nanoparticles in 3D printed monolithic multilayered microfluidic chip: enhanced chemiluminescence sensing predictions via machine learning algorithms. *Int. J. Biol. Macromol.* 245: 125502. https://doi.org/10.1016/j.ijbiomac.2023.125502.

14 Ansari, M.A., Kim, K.-Y., and Kim, S.M. (2018). Numerical and experimental study on mixing performances of simple and vortex micro T-mixers. *Micromachines* 9 (5): https://doi.org/10.3390/mi9050204.

15 Mahdavi, R., Hashemi-Najafabadi, S., Ghiass, M.A., and Adiels, C.B. (2024). Microfluidic design for in-vitro liver zonation – a numerical analysis using COMSOL multiphysics. *Med. Biol. Eng. Comput.* 62 (1): 121–133. https://doi.org/10.1007/s11517-023-02936-6.

16 Loganathan, A.K., Devaraj, R., and Krishnamoorthy, L. (2023). Revolutionizing plasma separation: cutting-edge design, simulation, and optimization techniques in microfluidics using COMSOL. *Microfluid. Nanofluidics* 27 (11): 73. https://doi.org/10.1007/s10404-023-02684-x.

17 Rananavare, M., Shah, R., Makwana, M., and Rathod, S.S. (2021). Design and simulation of microfluidic based carbon monoxide gas sensor using COMSOL Multiphysics®. In: *2021 International Conference on Advances in Computing, Communication, and Control (ICAC3)*, 1, 1–4, 4. Mumbai, India: IEEE https://doi.org/10.1109/ICAC353642.2021.9697247.

18 Soheili, S., Mandegar, E., Moradikhah, F. et al. (2021). Experimental and numerical studies on microfluidic preparation and engineering of chitosan nanoparticles. *J. Drug Deliv. Sci. Technol.* 61: 102268. https://doi.org/10.1016/j.jddst.2020.102268.

19 Zareei, S.M., Sepehrirahnama, S., Jamshidian, M., and Ziaei-Rad, S. (2023). Three-dimensional numerical simulation of particle acoustophoresis: COMSOL implementation and case studies. *Eng. Comput.* 39 (1): 735–750. https://doi.org/10.1007/s00366-022-01663-0.

20 Lin, X., Su, J., and Zhou, S. (2022). Microfluidic chip of concentration gradient and fluid shear stress on a single cell level. *Chin. Chem. Lett.* 33 (6): 3133–3138. https://doi.org/10.1016/j.cclet.2021.10.026.